

Extremely Small Two-Element Monopole Antenna for HF Band Applications

Jungsuek Oh, *Student Member, IEEE*, Jihun Choi, *Student Member, IEEE*, Fikadu T. Dagefu, *Student Member, IEEE*, and Kamal Sarabandi, *Fellow, IEEE*

Abstract—This paper presents a novel antenna architecture to achieve an extremely small form factor for HF band applications. The approach is based on manipulating the topology of a short monopole antenna without utilizing a high index material. A new architecture incorporating two radiating elements is configured, which allows significant gain enhancement. It is shown that such architecture can render a miniaturized HF antenna on air substrate having lateral and height dimensions as small as $0.0115\lambda_0 \times 0.0115\lambda_0 \times 0.0038\lambda_0$ ($150 \text{ mm} \times 150 \text{ mm} \times 50 \text{ mm}$ for operation at 22.9 MHz). It is found that the measured gain of such architecture can be as high as -18.1 dBi , which is 16.7 dB higher than a reference inverted-F antenna realized on a high index material ($\epsilon_R = 10.2$) having exactly the same dimensions. The proposed antenna architecture is composed of two in-phase radiating vertical elements connected to two inductors between which a capacitive top load is connected to achieve the desired resonant condition. The two vertical elements act effectively as a monopole having increased height. It is also shown that the gain of the antenna can be increased monotonically by increasing the quality factor (Q) of the phase shifter. High Q air-core inductors that can be accommodated in electrically small monopole antenna are designed and incorporated in the phase shifter to achieve a gain value of -17.9 dBi . Details about the proposed design approach, simulation, and measurement results are discussed.

Index Terms—Antenna gain, electrically small antennas, HF antennas, phase shifter, solenoids.

I. INTRODUCTION

EMERGING wireless technologies increase the needs for small-size, lightweight, and easily fabricated antennas. A quarter-wave monopole antenna is the most ubiquitous antenna used for many applications such as unattended ground sensors and ground-based communication systems at various frequency bands [1], [2]. However, the size of such antenna is prohibitively large for portable devices operating at low frequencies. This is particularly a major limiting factor at HF band whose applications for mobile wireless devices have been limited by the antenna size [3]–[5]. As a type of miniaturized monopole

antenna, low-profile inverted-F antennas (IFA) are most commonly used. One drawback of these antennas is that as their height decreases, the gain corresponding to vertically (co-)polarized radiation drops rapidly. This performance degradation is due to the increased power loss and the increase in radiated power from cross- (x-)polarized electric currents flowing on metallic traces highly concentrated and meandered in a small area [6], [7]. However, the horizontal currents are essential in establishing the required high current level on the short vertical pin, which is the main radiating component of the antennas [7]. In addition, many other types of low-profile electromagnetically coupled monopole antennas have been reported in the literature. In [8]–[13], capacitively loaded monopole antennas with different special disk geometries are presented for reducing the antenna height and improving the bandwidth. The height of these antennas is typically in the range of $\lambda_0/10$ with excellent operational bandwidth. However, their lateral dimensions are comparable to the wavelength. In [7], a new type of low-profile miniaturized monopole antenna utilizing inductive coupling and capacitive loading was reported. In this approach, significant size reduction ($\lambda_0/50 \times \lambda_0/16 \times \lambda_0/8$) is reported while polarization purity and high gain are maintained.

Recently, an antenna miniaturization technique using chip inductors has been investigated [14]–[16]. In [15] and [16], the chip inductors are embedded into the printed monopole antennas to decrease the size of the antennas at the expense of gain and bandwidth. To make the size of the antennas small enough for portable wireless devices, extreme miniaturization must be attempted when the typical size of the antennas is comparable to or smaller than $\lambda_0/100$. At these small dimensions, all antenna components act as lumped elements. Utilization of chip inductors and capacitors with poor quality factor for the antenna structure lowers radiation efficiency.

In this paper, a novel design for extremely small HF monopole antennas is presented. The proposed antenna utilizes two short vertical elements producing in-phase radiated fields. In this way, the effective height of the short dipole is increased without physically increasing the height. This leads to enhanced gain compared with a short monopole with the same height [17]. In order to achieve the in-phase radiated fields from electric currents flowing on the two vertical elements, a novel antenna topology using a modified T-type 180° phase shifter is introduced. It is shown that increasing the quality factor (Q) of the inductors used in the phase shifter can lead to significant gain enhancement. For example, it is shown that optimized air-core inductors can improve the gain by a factor of 14 ($= 11.3 \text{ dB}$) compared with a commercial chip inductor. The basic

Manuscript received May 16, 2012; revised December 03, 2012; accepted January 17, 2013. Date of publication February 25, 2013; date of current version May 29, 2013. This research was supported by the U.S. Army Research Laboratory under contract W911NF and prepared through collaborative participation in the Microelectronics Center of Micro Autonomous Systems and Technology (MAST) Collaborative Technology Alliance (CTA). The partial support from Global Photonic Energy Corporation is also acknowledged.

The authors are with The Radiation Laboratory, Department of Electrical Engineering and Computer Science, The University of Michigan at Ann Arbor, Ann Arbor, MI 48109-2122 USA (e-mail: jungsuek@umich.edu; sarabandi@eecs.umich.edu).

Digital Object Identifier 10.1109/TAP.2013.2249034

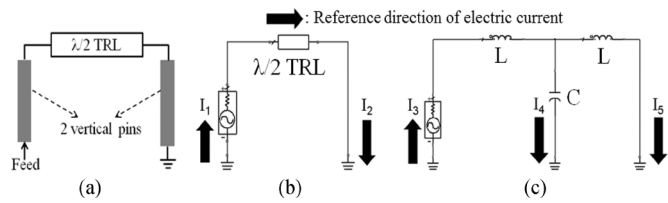


Fig. 1. (a) Two vertical elements put $\lambda_0/2$ away from each other, (b) its circuit model, and (c) a circuit model for the conventional T-type 180° phase shifter.

idea is presented in Section II. Design, implementation, and performance assessment of the proposed HF antenna using chip inductors are presented in Section III. In Section IV, we discuss gain enhancement using optimized air-core inductors and the approach for incorporating such inductors within the antenna volume. In Section V, the proximity effect of objects on the resonant frequency of the proposed antenna with narrow bandwidth is investigated.

II. REALIZATION OF TWO IN-PHASE RADIATING VERTICAL ELEMENTS USING A MODIFIED T-TYPE 180° PHASE SHIFTER

Let us imagine a short-circuited $\lambda_0/2$ transmission line (TRL) resonator connected to two shorting pins at both ends. Large electric currents on the two shorting pins can radiate vertically polarized fields that are in phase. Fig. 1(a) shows two vertical elements (pins) connected by a $\lambda_0/2$ TRL. Radiated fields from the electric currents flowing on the two vertical pins are in phase because of the 180° phase shift from the $\lambda_0/2$ TRL. The corresponding circuit model is shown in Fig. 1(b), assuming that small inductances from the two vertical pins with very low profile ($\ll \lambda_0/100$) can be ignored. The black arrow depicts the reference direction of the electric current at each probing position. To reduce the long lateral dimension of the $\lambda_0/2$ TRL, using a meandered metallic trace causes high ohmic loss, and increases x-polarized radiated fields. Therefore, the proposed antenna is designed to achieve the electric currents that can radiate in-phase using an alternative approach [7].

Instead of using the $\lambda_0/2$ TRL, a T-type 180° phase shifter with a capacitive impedance inverter can be used [17]. Fig. 1(c) shows the circuit model where $L = 10$ nH and $C = 9.6$ pF and the reference directions of electric currents on the vertical elements. Fig. 2 shows the magnitude and phase of I_1, I_2, I_3, I_4 and I_5 , which are highlighted in Fig. 1. As expected, at 23 MHz, I_1 and I_2 have the same magnitude but 180° phase difference. This corresponds to in-phase radiation from the vertical elements. However, Fig. 2(d) shows that the current in the capacitor branch flows in the opposite direction of the currents in the feed and shorting pins. The magnitude (0.08 A at 23 MHz) of I_4 is twice that (0.04 A at 23 MHz) of I_3 or I_5 , as shown in Fig. 2(c). Hence, the radiated fields from I_4 cancel out the radiated fields from I_3 and I_5 . To avoid this radiation cancellation, it is important to eliminate the conduction current path I_4 , while maintaining the 180° phase shift for I_5 .

The conduction current I_4 can be eliminated altogether by replacing the lumped capacitor with an open stub, as shown in Fig. 3(b). Characteristic impedance and length of the open stub in the circuit schematic are appropriately chosen to achieve the

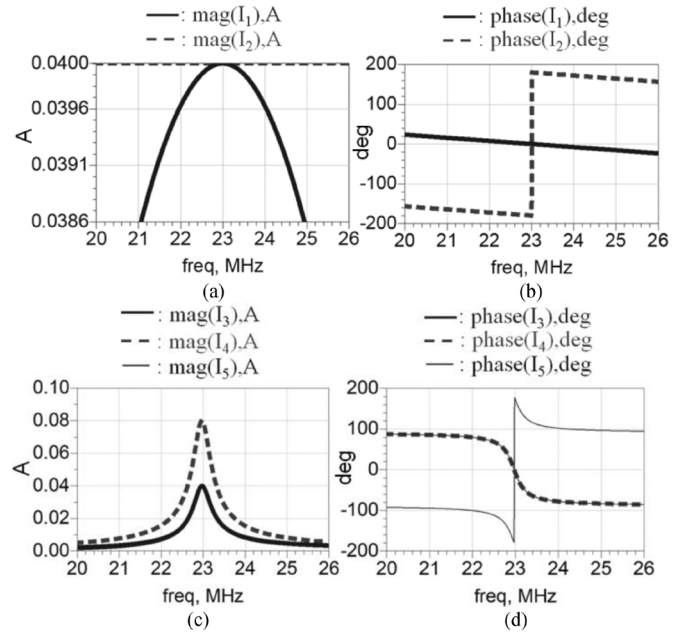


Fig. 2. (a) Magnitudes and (b) phases of I_1 and I_2 , and (c) magnitudes and (d) phases of I_3, I_4 and I_5 shown in Fig. 1.

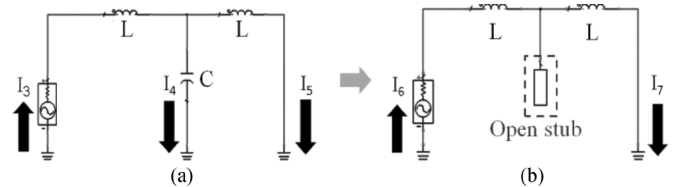


Fig. 3. (a) Circuit model for a T-type 180° phase shifter, and (b) circuit model employing an open stub instead of a grounded capacitor in (a).

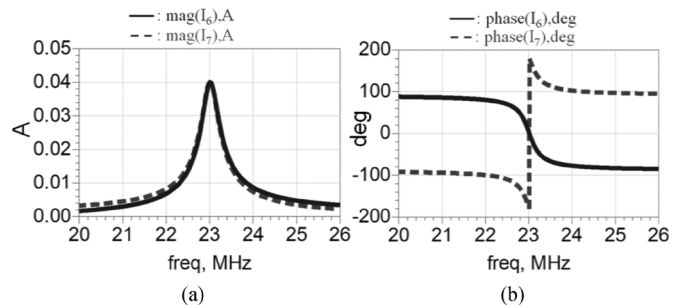


Fig. 4. (a) Magnitudes and (b) phases of I_6 and I_7 shown in Fig. 3.

required 180° phase shift at 23 MHz. Fig. 4 shows the magnitudes and phases of I_6 and I_7 , indicating the same magnitude and 180° phase difference for achieving efficient vertically polarized radiation.

III. EXTREMELY SMALL TWO-ELEMENT MONOPOLE ANTENNA CONFIGURATION

A. Antenna Design

Based on the equivalent circuit model shown in Fig. 3(b), an extremely low-profile miniaturized HF antenna with two in-phase radiating vertical elements is designed. Fig. 5 shows the side view and the top view of the proposed antenna. The

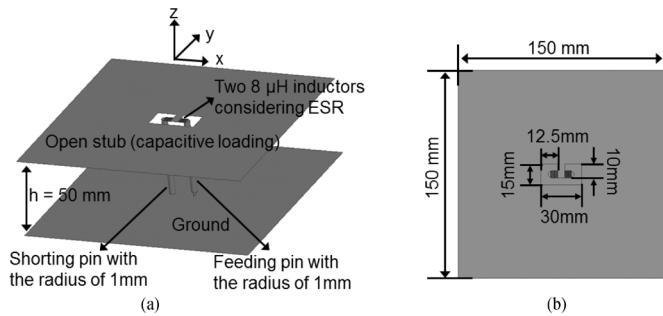


Fig. 5. (a) Side view and (b) top view of the proposed antenna with chip inductors.

lateral dimension and height of the proposed antenna, including the ground plane, are 150 mm ($0.0115\lambda_0$) and 50 mm ($0.0038\lambda_0$), respectively. The top metallic plate acts as the open stub (capacitor of the phase shifter) connected between the two chip inductors ($8\ \mu\text{H}$, part number: 1812CS-822XJLB by *coilcraft*), which are connected to the vertical pins. The substrate used in this design is air, allowing elimination of dielectric loss from the antenna structure. In order to include ohmic loss in the simulation, the finite conductivity of copper is used in all metallic traces and the two vertical pins. In order to consider actual characteristics of the chip inductors, equivalent series resistance (ESR) of $28\ \Omega$ is extracted at 23 MHz from the datasheet provided by the manufacturer [18]. The ESR is included in the simulation for calculation of antenna input impedance and radiation efficiency. By optimizing the distance between the shorting pin and the feeding pin appropriately, impedance matching to a $50\ \Omega$ feed is obtained. The geometry of the open stub on the top plate is chosen to be symmetric in terms of xz and yz planes, and the positions of the two pins are chosen near the center of antenna structure to obtain omnidirectional radiation pattern.

Fig. 6(a) shows the simulated S_{11} of the proposed antenna with the center frequency of 23.2 MHz. It should be noted that using a coaxial feed cable to measure S_{11} of the monopole antennas having a very small ground plane ($0.0115\lambda_0 \times 0.0115\lambda_0$) produces incorrect results. This is due to the strong near-field coupling between the antenna and outer conductor of the coaxial cable. The excited induced currents over the cable produces changes in radiation pattern and S_{11} [7]. To avoid this measurement problem, a small source module can be connected to the antenna feed. Fig. 7 shows the fabricated antenna integrated with the small source module consisting of a voltage controlled oscillator (VCO), potentiometer, and a 12-V battery. By controlling the potentiometer, the bias voltage of the VCO can be changed, enabling frequency tuning. By observing the variation of received power versus frequency, the operating (resonant) frequency of the antenna is found. This is done using the proposed antenna with chip inductors as a transmitting antenna and using a $\lambda_0/10$ dipole antenna with a wider bandwidth as a receiving antenna.

Fig. 6(b) shows the setup used to measure the received power and the radiation patterns of the proposed antenna. The transmitting antenna (the proposed antenna) is mounted on a positioner, and the receiving antenna ($\lambda_0/10$ dipole antenna) is mounted in

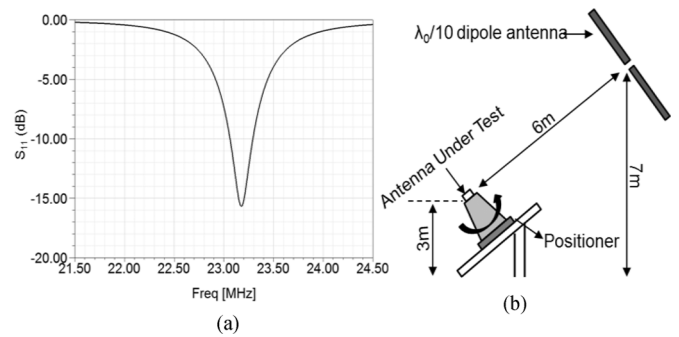


Fig. 6. (a) Simulated S_{11} of the proposed antenna with chip inductors and (b) measurement setup in an elevated antenna range.

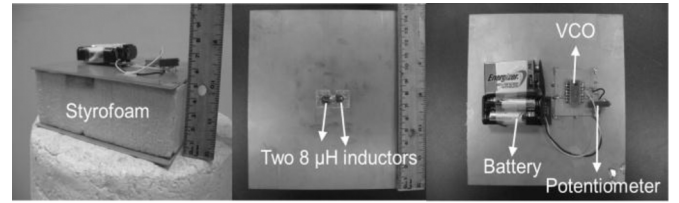


Fig. 7. Fabricated antenna with chip inductors, integrated with the source module.

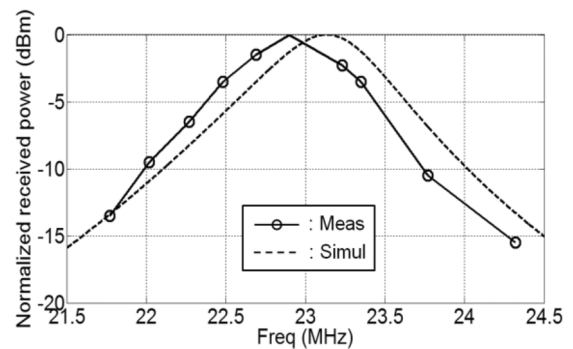


Fig. 8. Measured and simulated power received at the reference $\lambda_0/10$ dipole antenna and normalized by the peak value of each response versus frequency when the proposed antenna with chip inductors is used as a transmitting antenna.

an elevated position. By using this elevated range, the measurement error caused by the reflected waves from the ground can be decreased substantially. In order to calculate the measured gain of the proposed antenna, two $\lambda_0/10$ dipole antennas are used, as reference antennas. As a substitution method, from three different configurations of Tx and Rx antennas using the three antennas with unknown gain, the gain of the proposed antenna can be derived. As mentioned earlier, S_{11} of the proposed antenna cannot be measured directly by a network analyzer due to the near-field coupling. However, it can be indirectly evaluated by comparing the slope and the center frequency of the measured received power versus frequency to those of the simulated response. Fig. 8 shows measured and simulated power received by the $\lambda_0/10$ dipole antenna in an elevated range versus frequency. The power is normalized by the peak value of each plot for a better slope comparison between the measured and simulated plots. It is shown that the slope of the measured plot is similar to that of the simulated plot, indicating that S_{11} of the fabricated

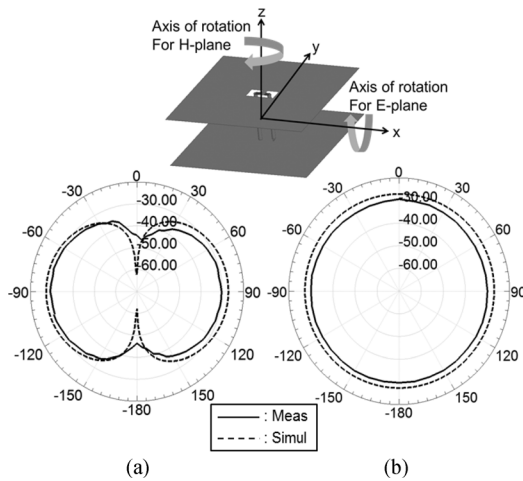


Fig. 9. Measured and simulated radiation patterns of the proposed antenna with chip inductors in the (a) E- (yz) plane and (b) H- (xy) plane.

antenna is well matched to the simulated S_{11} . The measured resonant frequency is 22.9 MHz, which is slightly shifted from the simulated resonant frequency of 23.2 MHz due to the 5% tolerance range of the commercial chip inductors. Fig. 9 shows measured and simulated radiation patterns in the E- (yz) plane and H- (xy) plane. Omnidirectional radiation pattern is observed in the H-plane. The measured antenna gain is -29.2 dBi, which is similar to the simulated gain of -28.1 dBi.

B. Gain and Mass Comparison

To examine a figure of merit of the proposed antenna, its gain and mass are compared with those of a conventional inverted-F antenna having the same dimensions and volume. A small inverted-F antenna can be fabricated using a $\lambda_0/4$ open-ended transmission line on a high index substrate material. The free-space wavelength (λ_0) at 22.9 MHz is 13.1 m, and thus $\lambda_0/4$ is 3.275 m. Fitting a $\lambda_0/4$ inverted-F antenna on very small area of $150 \text{ mm} \times 150 \text{ mm}$ ($0.0115\lambda_0 \times 0.0115\lambda_0$) is not practical. Thus, the use of a substrate with high dielectric constant ($\epsilon_R = 10.2$ and $\tan \delta = 0.002$) is necessary. A spiral geometry is used to accommodate the quarter-wave transmission line as shown in Fig. 10. Fig. 11 shows the simulated S_{11} of the spiral-shaped inverted-F antenna, compared with that of the proposed two-element short monopole antenna. It is found that the 10-dB return loss bandwidth of the spiral-shaped IFA is much narrower than that of the proposed antenna due to the highly stored electric energy in the high dielectric substrate. Fig. 12 shows the simulated radiation patterns in the E-plane and H-plane of the spiral-shaped IFA. The gain of the spiral-shaped IFA is calculated as -34.6 dBi, which is 5.4 dB lower than the measured gain of the proposed antenna. This is due to the ohmic loss in the spiral trace and dielectric losses, despite a very good dielectric loss tangent ($\tan \delta = 0.002$). This result suggests that the parasitic losses from the two chip inductors in the proposed antenna are much lower than the ohmic and dielectric losses in the spiral-shaped IFA. It is also found that the proposed two-element short monopole antenna provides wider bandwidth than the spiral-shaped IFA.

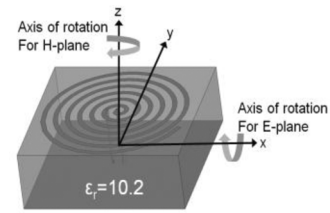


Fig. 10. Spiral-shaped inverted-F antenna on the substrate with $\epsilon_R = 10.2$.

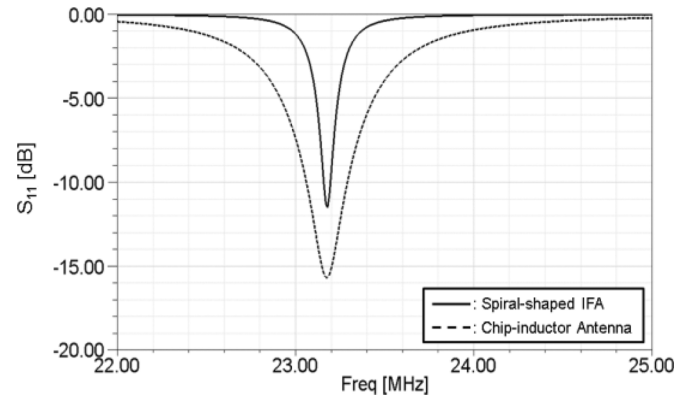


Fig. 11. Simulated S_{11} of spiral-shaped inverted-F antenna on the substrate with $\epsilon_R = 10.2$, compared with that of the proposed antenna with chip inductors.

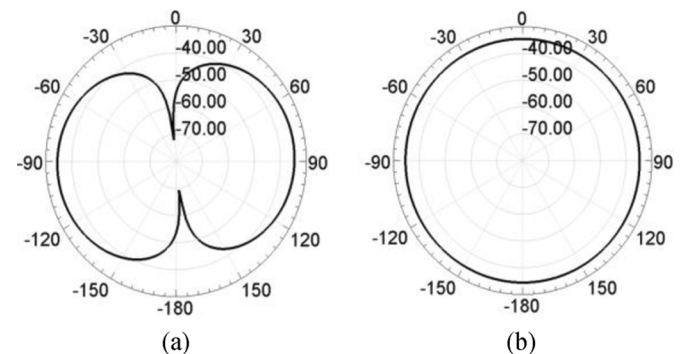


Fig. 12. Simulated radiation patterns of spiral-shaped inverted-F antenna on the substrate with $\epsilon_R = 10.2$ in the (a) E(yz) plane and (b) H(xy) plane.

Another advantage of the proposed two-element short monopole antenna over the IFA is its much lower mass. The substrate materials with high dielectric-constant usually have high mass density, which makes the antenna that uses such substrates heavy. The proposed antenna provides miniaturization without the need for high index materials, and thus it can be made very light. Table I shows the masses of all the materials used to fabricate the spiral-shaped IFA with a substrate having $\epsilon_R = 10.2$ and the proposed antenna with air substrate. The total mass of the conventional inverted-F antenna (3502 g) is about 220 times heavier than that of the proposed antenna (15.8 g). Fig. 13 shows the proposed antenna fabricated using flexible thin substrates.

TABLE I
MASS OF EACH PART OF THE PROPOSED ANTENNA WITH
AIR SUBSTRATE AND THE SPIRAL-SHAPED INVERTED-F
ANTENNA ON THE SUBSTRATE WITH $\epsilon_r = 10.2$

Inverted-F antenna (g) on the substrate ($\epsilon_r=10.2$)		The proposed antenna (g)	
One 50mm RO6010	3501	Two 50um ULTRALAM 3850 LCP	13.293
		Styrofoam to support a top-plate	0.352
Two inductors	0.1	Two inductors	0.1
One copper post	1.4	Two copper posts	2.02
Total mass (g)	3502		15.8

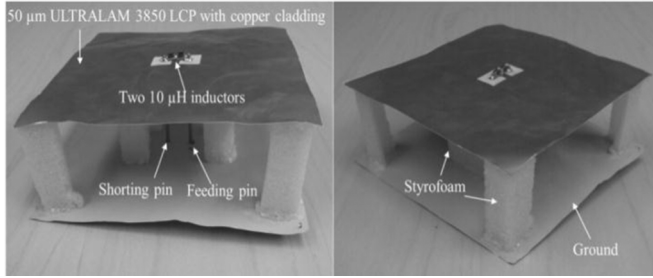


Fig. 13. Proposed antenna fabricated using flexible thin substrates.

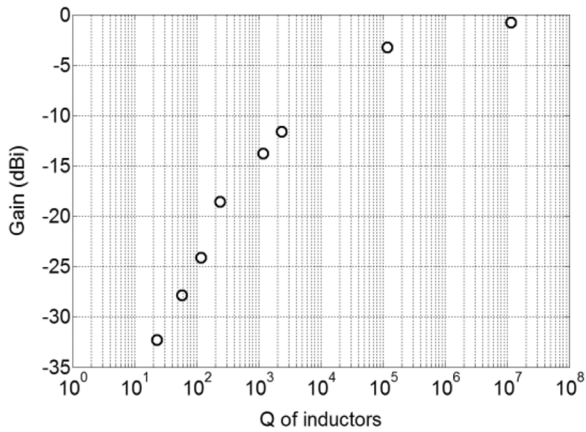


Fig. 14. Simulated gains of the proposed antennas with chip inductors versus Q of the chip inductors.

IV. GAIN ENHANCEMENT USING OPTIMIZED AIR-CORE INDUCTORS

As discussed in Section III-B, the proposed two-element antenna provides higher gain than the conventional spiral-shaped IFA. This section shows that further gain enhancement can be achieved by increasing the Q of the inductors used in the phase shifter. This is possible because the Q of the commercial chip inductor is rather low ($Q = 45$). Fig. 14 shows simulated gain of the proposed antenna versus Q of the inductors. It indicates that increasing Q of the chip inductors from 45 to 450 can lead to gain enhancement of about 10 dB. The relationship between the gain and Q of the inductors is almost linear up to about $Q \approx 10^4$. Beyond the value, radiation resistance in the proposed antenna dominates over losses on the metallic surfaces. The gain will saturate to the gain of the ideal short dipole (1.76 dBi) if one were to ignore metallic losses.

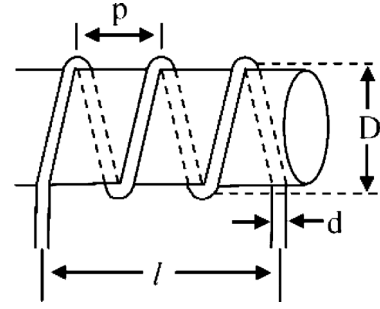


Fig. 15. Design parameters of the air-core coil.

It is reported that Q of air-core inductors can be as high as several hundred at HF band due to the absence of the ferrite core loss [19]–[23]. In this section, design and performance of an extremely small two-element monopole antenna using air-core inductors are discussed. Since air-core coils have lower inductance values than the ferromagnetic core coils, the size of the inductors must be increased. Therefore, the most important design issue determining antenna gain is to optimize Q of air-core inductors restricted by the size of the antenna.

A. Optimization of Quality Factor of Air-Core Inductors

The Q of an air-core inductor is determined by two loss mechanisms related to proximity effect and skin effect. The proximity effect refers to the concentration of electric currents on a small portion of wires due to the proximity of the adjacent wires in the inductor coil. This proximity effect can significantly increase ac resistance of adjacent conductors when compared to its dc resistance. The adverse proximity effect on the ac resistance increases with frequency. At higher frequencies, the ac resistance of a conductor can easily exceed ten times its dc resistance [24]. Recently, methods for accurate prediction of inductance and ac resistance of coils at high frequencies have been reported [25], [26]. In [25], the coil is analytically modeled as a slow-wave anisotropic waveguide and analytic formulas to determine the inductance and ac resistance are presented. The formulas are corrected based on experimental data as presented in [26] and [27]. Fig. 15 shows design parameters of the coil, and (1) and (2) are the analytic formulas, including the correction factor derived from experimental data to calculate the inductance and ac resistance.

Based on the literatures, the inductance is given by

$$L = (\mu_0 \pi D^2 N^2 k_L / 4l) - [\mu_0 D N (k_{S(e)} + k_m) / 2] + L_I \quad (1)$$

where D is the effective current-sheet diameter, N is the number of turns, l is the coil length, L_I is the internal inductance, k_L is Nagaoka's coefficient, k_m is Rosa's mutual-inductance correction term presented in [26], and $k_{S(e)} = (3/2) - \ln(2p/d)$ where d is the diameter of the wire and p is the winding pitch-distance.

The ac resistance is given by

$$R_{ac} = R_{dc} [1 + (\Omega - 1) \psi (N - 1 + 1/\psi) / N] \quad (2)$$

where R_{dc} is dc resistance, ψ is proximity factor (derived by the interpolation of Medhurst's table of experimental data [27]) and $\Omega = D^2 / [4(D\delta_I - \delta_I^2)]$, where $\delta_I = \text{skin depth}$.

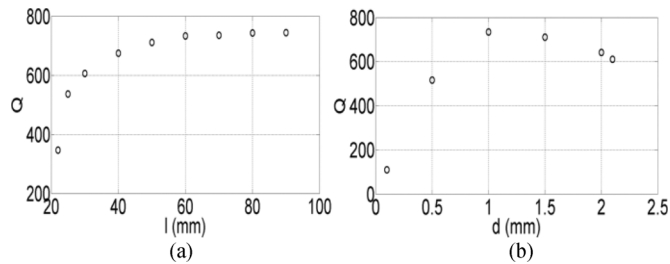


Fig. 16. Calculated Q versus (a) l (= coil length) where $D = 1$ mm, and (b) D (= wire diameter), where $l = 70$ mm.

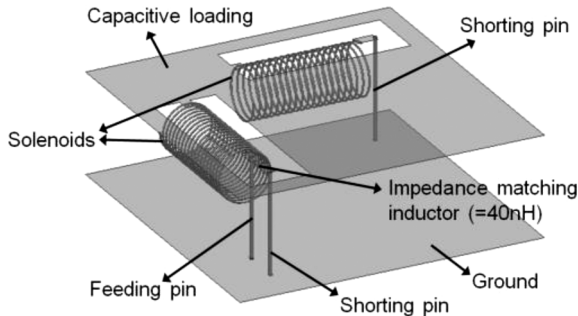


Fig. 17. Geometry of the proposed antenna with air-core inductors having the dimensions of $150 \text{ mm} \times 150 \text{ mm} \times 50 \text{ mm}$.

Based on (1) and (2), dimension parameters of an air-core solenoid with inductance of $8 \mu\text{H}$ are optimized considering the constrained antenna volume of $150 \text{ mm} \times 150 \text{ mm} \times 50 \text{ mm}$. In order not to increase vertical profile of the antenna, the coil is placed between the ground plane and the top plate, which limits the diameter of the coil to be strictly smaller than 50 mm . In the proposed antenna, 25 mm is chosen for the coil diameter in order not to drastically increase the top plate capacitance. With the fixed coil diameter (D), the effects of coil length (l) and wire diameter (d) on Q are investigated. Once the values of D and l (or d) are chosen and fixed, the values of other parameters such as the number of turns (N) and the winding pitch-distance (p) are accordingly determined to achieve the required inductance of $8 \mu\text{H}$. Fig. 16(a) shows the calculated Q versus l where d is 1 mm . This figure suggests that increasing l after about $l = 60 \text{ mm}$ does not affect Q of the inductor. This is due to the fact that the proximity effect vanishes once wires are far from each other (large p). 70 mm is chosen as the optimum value of l . With the chosen $l = 70 \text{ mm}$, the effect of d is iteratively examined. Fig. 16(b) shows Q versus d , where l is 70 mm . The figure suggests that increasing d beyond $D = 1 \text{ mm}$, the Q of the inductors decreases because p decreases with fixed l , leading to the increase in the proximity effect. Finally, the values of D , N , l , d , and p are chosen as 25 mm , 32 , 70 mm , 1 mm and 2.3 mm , respectively, resulting in a quality factor of about 730 .

B. Antenna Design

The air-core solenoids designed in the previous section are used to design an extremely small two-element monopole antenna. Fig. 17 shows the geometry of the proposed antenna with the same dimensions as the previous antenna where chip inductors were used. As mentioned earlier, the solenoids are inte-

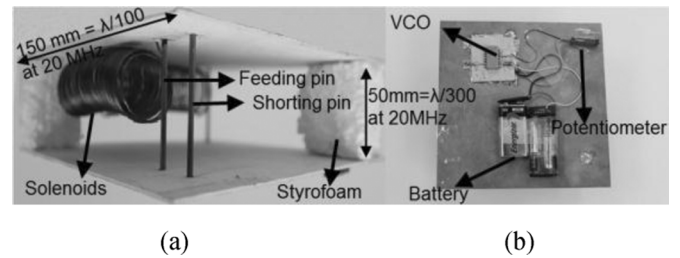


Fig. 18. (a) Side view and (b) bottom view of the fabricated antenna incorporating air-core inductors, integrated with the source module.

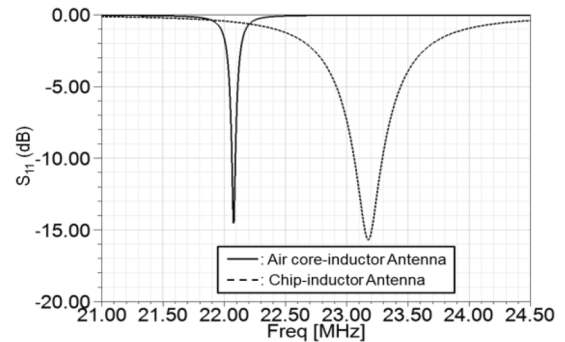


Fig. 19. Simulated S_{11} of the proposed antenna with air-core inductors, compared to that of the antenna with chip inductors. Narrower bandwidth indicates higher radiation efficiency because the antenna volume is fixed.

grated underneath the capacitive loading plate not to increase the overall vertical profile of the antenna. The copper layer over the area where the solenoids are positioned is removed to reduce the effect of the top metallic plate on the inductance and the effect of the solenoids on the top plate capacitance. An additional shunting pin with a chip inductor of 40 nH is used to get impedance matching to a $50\text{-}\Omega$ feed. This is similar to the use of a vertical element positioned close to a feeding element in the conventional inverted-F antenna for the impedance matching. In this usage, the magnitude of the electric current on the additional vertical element is much smaller than that of the electric element on the other vertical elements, and thus the radiation from the new vertical element is negligible. Fig. 18 shows the side and bottom view of the fabricated antenna integrated with the source module.

Fig. 19 shows the simulated S_{11} of the antenna with air-core inductors, compared to that of the antenna with chip inductors. As expected, the bandwidth of the antenna with air-core inductors is narrower than that of the antenna with chip inductors due to very high Q (730) of the air-core inductors. As discussed in Section III-A, S_{11} of the proposed antenna cannot be measured directly by a network analyzer due to the aforementioned near-field coupling. As before, the center frequency and the bandwidth are characterized through transmission measurement. Fig. 20 shows the measured and simulated power received at the reference $\lambda_0/10$ antenna as a function of frequency. The power is normalized by the peak value of each response to compare the different plots. It is shown that the slope of the measured response of the antenna with air-core inductors is much steeper than that of the antenna with chip inductors, showing

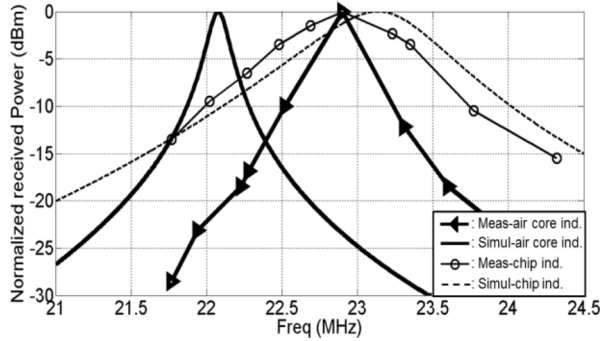


Fig. 20. Measured and simulated power received at the reference $\lambda_0/10$ antenna and normalized by the peak value of each response versus frequency when the proposed antenna with air-core inductors is used as a transmitting antenna, compared with those of the antenna with chip inductors.

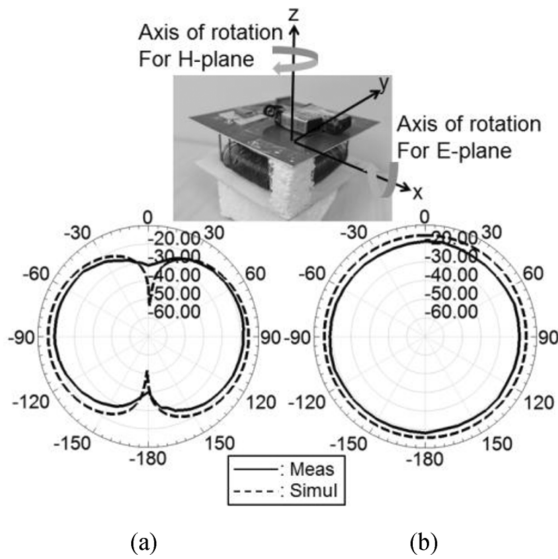


Fig. 21. Measured and simulated radiation patterns of the proposed antenna with air-core inductors in the (a) $E(=yz)$ plane and (b) $H(=xy)$ plane.

good agreement with the simulated plot. Measured resonant frequency is 22.9 MHz, which is slightly different from the simulated resonant frequency of 22.1 MHz due to the interaction between the solenoids and other metallic parts. Fig. 21 shows the measured and simulated radiation patterns in the $E(=yz)$ plane and $H(=xy)$ plane. Omnidirectional radiation pattern is observed in the H-plane and measured antenna gain is found to be -17.9 dBi. This is 11.3 and 16.7 dB higher than that of the antenna with chip inductors and the spiral-shaped IFA, respectively. The total mass of the antenna with two air-core solenoids made of copper is 51.95 g.

Since the sizes of the antennas under discussion are electrically very small, it is interesting to compare the performance of the antennas to the fundamental limit derived by [28]. To do that, a figure of merit is used, defined as the product of the 3-dB return loss bandwidth (BW) and radiation efficiency (η). Fig. 22 shows the figures of merit corresponding to the antennas, electrical small antennas in literature and the fundamental limit. The 3-dB return loss bandwidth (BW) of the fundamental limit is calculated using $BW = 1/Q$ where $Q \approx 1/(kr)^3$ where k is the wavenumber, and r is the radius of the smallest sphere

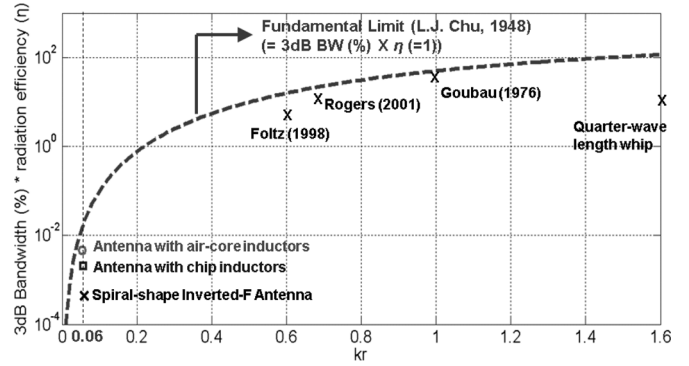


Fig. 22. Performance comparison among electrically small antennas introduced in this paper and other literature.

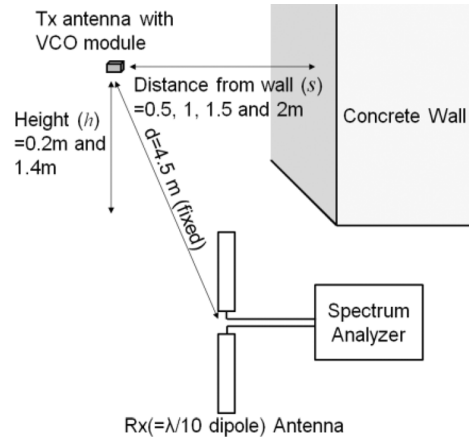


Fig. 23. Measurement set up for examining the proximity effect of nearby objects on the resonant frequency of the proposed narrow band antenna.

that can enclose the antenna. The results suggest that although the bandwidth of the antenna with air-core inductors is narrower than those of the antenna with chip inductors and the spiral-shaped IFA, because the radiation efficiency of the antenna with air-core inductors is tens of times higher than those of others, the figure of merit of the antenna with air-core inductors gets much closer to the fundamental limit than the other antennas. With this analysis, it is successfully validated that the proposed electrically small antenna provides significantly enhanced performance, compared to the conventional IFA.

V. PROXIMITY EFFECT OF NEARBY OBJECTS

For very small antennas with narrow bandwidth, there is always a concern about the proximity effect of nearby objects as regards the possible shift in resonant frequency. At HF band where the wavelength is large, typical distances between the small antennas and nearby objects in an indoor environment are very small compared with the wavelength. In order to examine the feasibility of using the proposed antennas for such environments, the change in the operating frequency caused by nearby objects is investigated. This is done experimentally by changing the distance between the antenna and a concrete wall, and the ground in an indoor environment. Fig. 23 shows the measurement set up. At wall separation distance (s) = 0.5, 1, 1.5 and 2 m, and ground height (h) = 0.2 m and 1.4 m, the power received at the $\lambda_0/10$ dipole antenna is measured and normalized

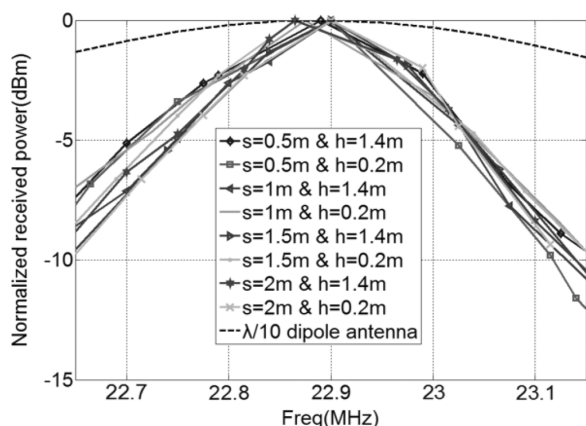


Fig. 24. Measured received normalized power corresponding to various positions of the transmitting (= proposed) antenna shown in Fig. 23.

by the peak value of each plot when the proposed antenna with air-core inductors is used as a transmitting antenna.

Fig. 24 shows the measurement results, indicating a stable operating frequency of the proposed antenna. The small variation observed is due to frequency jitter of the VCO itself. Also the frequency response of a $\lambda_0/10$ dipole antenna as the transmitting antenna when the same $\lambda_0/10$ dipole antenna is used as the receiving antenna is shown to indicate that the observed steep frequency response is due to the frequency response of the proposed two-element monopole antenna.

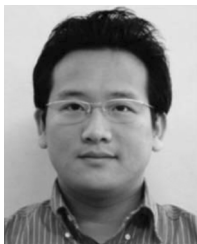
VI. CONCLUSION

A new type of extremely small two-element monopole antenna with vertical polarization and omnidirectional radiation pattern is presented. The antenna has a very small form factor and fits in a very small volume having dimensions $(0.0115\lambda_0 \times 0.0038\lambda_0 \times 0.0038\lambda_0)$. The basic idea is to feed two short monopoles connected by a modified 180° phase shifter. In this way, the effective height of the antenna is increased which leads to high radiation efficiency. The phase shifter is a T-type inductor-capacitor-inductor element modified by replacing the grounded capacitor with a capacitive stub. With this modification, no opposing vertical conduction current exists on the antenna structure. This design is further improved by minimizing the power loss from the antennas by using high Q air-core inductors. A novel antenna with air-core inductors exhibiting 16.7 dB higher gain than the conventional spiral-shaped inverted-F antenna on a high index substrate material ($\epsilon_R = 10.2$) is presented. The enhanced gain of the proposed antennas and the feasibility of using them with nearby objects are demonstrated.

REFERENCES

- [1] P. L. Werner and D. H. Werner, "Design synthesis of miniature multi-band monopole antennas with application to ground-based and vehicular communication systems," *IEEE Antennas Wireless Propag. Lett.*, vol. 4, pp. 104–106, 2005.
- [2] D. Liao and K. Sarabandi, "Optimization of low-profile antennas for applications in unattended ground sensor networks," *IEEE Trans. Antennas Propag.*, vol. 53, no. 11, pp. 3747–3756, Nov. 2005.

- [3] J. Baker, H. S. Youn, N. Celik, and M. F. Iskander, "Low-profile multifrequency HF antenna design for coastal radar applications," *IEEE Antennas Wireless Propag. Lett.*, vol. 9, pp. 1119–1122, 2010.
- [4] P. L. Chi, R. Waterhouse, and T. Itoh, "Antenna miniaturization using slow wave enhancement factor from loaded transmission line models," *IEEE Trans. Antennas Propag.*, vol. 59, pp. 48–57, Jan. 2011.
- [5] F. T. Dagefu, J. Oh, and K. Sarabandi, "A sub-wavelength RF source tracking system for GPS-denied environments," *IEEE Trans. Antennas Propag.*, vol. 61, no. 4, pp. 2252–2262, Apr. 2013.
- [6] W. B. Hong and K. Sarabandi, "Low-profile, multi-element, miniaturized monopole antenna," *IEEE Trans. Antennas Propag.*, vol. 57, no. 1, pp. 72–80, Jan. 2009.
- [7] J. Oh and K. Sarabandi, "Low profile, miniaturized, inductively coupled capacitively loaded monopole antenna," *IEEE Trans. Antennas Propag.*, vol. 60, no. 3, pp. 1206–1213, Mar. 2012.
- [8] J. McLean, H. Foltz, and G. Crook, "Broadband, robust, low profile monopole incorporating top loading, dielectric loading, and a distributed capacitive feed mechanism," in *Proc. IEEE Int. Symp. Antennas Propag.*, Jul. 11–16, 1999, vol. 3, pp. 1562–1565.
- [9] S. Tokumaru, "Multiplates: Low profile antennas," in *Proc. IEEE Int. Symp. Antennas Propag.*, Oct. 1976, vol. 14, pp. 379–382.
- [10] N. Herscovici and E. Dziadek, "Omnidirectional antennas for wireless communication," in *Proc. IEEE Int. Symp. Antennas Propag.*, Jul. 11–16, 1999, vol. 1, pp. 556–559.
- [11] T. Noro and Y. Kazama, "Low profile and wide bandwidth characteristics of top loaded monopole antenna with shorting post," in *Proc. IEEE Int. Workshop Antenna Technol., Small Antennas, Novel Metamater.*, Mar. 6–8, 2006, pp. 108–111.
- [12] C. Delaveaud, P. Levegue, and B. Jecko, "Small-sized low-profile antenna to replace monopole antennas," *Electron. Lett.*, vol. 34, pp. 716–717, Apr. 1998.
- [13] G. Goubau, "Multielement monopole antennas," in *Proc. Workshop Electrically Small Antennas ECOM*, Ft. Monmouth, NJ, May 1976, pp. 63–67.
- [14] Q. Luo, J. R. Pereira, and H. M. Salgado, "Compact printed monopole antenna with chip inductor for WLAN," *IEEE Antennas Wireless Propag. Lett.*, vol. 10, pp. 880–883, 2011.
- [15] K. Wong and S. Chen, "Printed single-strip monopole using a chip inductor for penta-band WWAN operation in the mobile phone," *IEEE Trans. Antennas Propag.*, vol. 58, no. 3, pp. 1011–1014, Mar. 2010.
- [16] T. Kang and K. Wong, "Chip-inductor-embedded small-size printed strip monopole for WWAN operation in the mobile phone," *Microw. Opt. Technol. Lett.*, vol. 51, no. 4, pp. 996–971, Apr. 2009.
- [17] J. Oh and K. Sarabandi, "A low-profile omnidirectional planar antenna with vertical polarization employing two in-phase elements," in *Proc. Gen. Assembly Sc. Symp., 2011 XXXth URSI*, Aug. 13–20, 2011, pp. 1–4.
- [18] Coilcraft, Inc. [Online]. Available: <http://www.coilcraft.com/>
- [19] Y.-J. Kim and M. G. Allen, "Surface micromachined solenoid inductors for high frequency applications," *IEEE Trans. Compon., Packag., Manuf. Technol.*, vol. 21, pp. 26–33, Jan. 1998.
- [20] C. R. Sullivan, L. Weidong, S. Prabhakaran, and L. Shanshan, "Design and fabrication of low-loss toroidal air-core inductors," in *Proc. Power Electron. Spec. Conf. 2007*, pp. 1754–1759.
- [21] S. C. Tang, S. Y. R. Hui, and H. Chung, "Coreless planar printed-circuit board (PCB) transformers—A fundamental concept for signal and energy transfer," *IEEE Trans. Power Electron.*, vol. 15, no. 5, pp. 931–941, Sep. 2000.
- [22] S. Y. R. Hui, S. C. Tang, and H. Chung, "Some electromagnetic aspects of coreless PCB transformers," *IEEE Trans. Power Electron.*, vol. 15, no. 4, pp. 805–810, Jul. 2000.
- [23] S. C. Tang, S. Y. R. Hui, and H. Chung, "Characterization of coreless printed circuit board (PCB) transformers," *IEEE Trans. Power Electron.*, vol. 15, no. 6, pp. 1275–1282, Nov. 2000.
- [24] P. Dowell, "Effects of eddy currents in transformer windings," in *Proc. Inst. Electr. Eng.*, Aug. 1966, vol. 113, pp. 1387–1394.
- [25] K. L. Corum and J. F. Corum, "RF coils, helical resonators and voltage magnification by coherent spatial modes," *IEEE Microw. Rev.*, vol. 7, no. 2, pp. 36–45, Sep. 2001.
- [26] W. Knight David, "Rosa's mutual inductance correction for the round-wire solenoid," G3YNH [Online]. Available: http://www.g3ynh.info/zdocs/magnetics/appendix/Rosa/Rosa_km.pdf
- [27] R. G. Medhurst, "H. F. resistance and self-capacitance of single-layer solenoids," *Wireless Eng.*, pp. 80–92, Mar. 1947.
- [28] L. J. Chu, "Physical limitations on omnidirectional antennas," *J. Appl. Phys.*, vol. 19, pp. 1163–1175, Dec. 1948.



Jungsuek Oh (S'08) received the B.S. and M.S. degrees from Seoul National University, Seoul, Korea, in 2002 and 2007, respectively, and the Ph.D. degree from the University of Michigan at Ann Arbor, MI, USA, in 2012.

From 2007 to 2008, he was an Associate Research Engineer with Korea Telecom, working on the development of flexible RF devices. He is currently a Research Fellow with the Radiation Laboratory, University of Michigan. His research areas include antenna miniaturization for integrated systems and radio propagation modeling for indoor scenarios. He has published more than 25 journals and conference papers and has several patents on similar subjects.

Dr. Oh is the recipient of the 2011 Rackham Predoctoral Fellowship Award at the University of Michigan.



Jihun Choi (S'12) received the B.S. degree in electrical engineering from University of Incheon, Korea, in 2010.

Currently, he is working toward the M.S. degree in electrical engineering from the University of Michigan at Ann Arbor, MI, USA. Since 2011, he has been with the Radiation Laboratory, Department of Electrical Engineering, University of Michigan, where he is currently a Graduate Research Assistant.



Fikadu T. Dagefu (S'07) received the B.S. degree in electrical engineering from the University of Texas at Austin, TX, USA, in 2007 and the M.S. and Ph.D. degrees, both in electrical engineering, from The University of Michigan at Ann Arbor, MI, USA, in 2009 and 2012, respectively.

His research interests include physics-based wave propagation modeling and measurements, radar remote sensing, RF source tracking in GPS-denied environments, antenna diversity and low power HF communication with miniaturized antennas.

Dr. Dagefu is the recipient of the 2011 MIT Lincoln Laboratory Graduate Fellowship. He is a member of the Eta Kappa Nu and Tau Beta Pi honor societies. He was a finalist in the student paper competitions at the IEEE IGARSS international conference in 2009 and 2010.



Kamal Sarabandi (S'87–M'90–SM'92–F'00) received the B.S. degree in electrical engineering from the Sharif University of Technology, Tehran, Iran, in 1980, the M.S. degree in electrical engineering in 1986, and the M.S. degree in mathematics and the Ph.D. degree in electrical engineering from The University of Michigan at Ann Arbor, MI, USA, in 1989.

He is currently the Director of the Radiation Laboratory and the Rufus S. Teesdale Professor of Engineering in the Department of Electrical Engineering and Computer Science, The University of Michigan at Ann Arbor. His research areas of interest include microwave and millimeter-wave radar remote sensing, meta-materials, electromagnetic wave propagation, and antenna miniaturization. He possesses 25 years of experience with wave propagation in random media, communication channel modeling, microwave sensors, and radar systems and leads a large research group, including two research scientists and 16 Ph.D. students. He has graduated 40 Ph.D. and supervised numerous post-doctoral students. He has served as the Principal Investigator on many projects sponsored by the National Aeronautics and Space Administration (NASA), Jet Propulsion Laboratory (JPL), Army Research Office (ARO), Office of Naval Research (ONR), Army Research Laboratory (ARL), National Science Foundation (NSF), Defense Advanced Research Projects Agency (DARPA), and a large number of industries. Currently, he is leading the Center for Microelectronics and Sensors funded by the Army Research Laboratory under the Micro-Autonomous Systems and Technology (MAST) Collaborative Technology Alliance (CTA) program. He has published many book chapters and more than 220 papers in refereed journals on miniaturized and on-chip antennas, meta-materials, electromagnetic scattering, wireless channel modeling, random media modeling, microwave measurement techniques, radar calibration, inverse scattering problems, and microwave sensors. He has also had more than 500 papers and invited presentations in many national and international conferences and symposia on similar subjects.

Dr. Sarabandi served as a member of NASA Advisory Council appointed by the NASA Administrator for two consecutive terms from 2006 to 2010. He is serving as a Vice-President of the IEEE Geoscience and Remote Sensing Society (GRSS) and is a member of the Editorial Board of the PROCEEDINGS OF THE IEEE. He was an Associate Editor of the IEEE TRANSACTIONS ON ANTENNAS AND PROPAGATION and the IEEE SENSORS JOURNAL. He is a member of Commissions F and D of URSI. He was the recipient of the Henry Russel Award from the Regent of The University of Michigan. In 1999, he received a GAAC Distinguished Lecturer Award from the German Federal Ministry for Education, Science, and Technology. He was also a recipient of the 1996 EECS Department Teaching Excellence Award and a 2004 College of Engineering Research Excellence Award. In 2005, he received the IEEE GRSS Distinguished Achievement Award and the University of Michigan Faculty Recognition Award. He also received the best paper Award at the 2006 Army Science Conference. In 2008, he was awarded a Humboldt Research Award from The Alexander von Humboldt Foundation of Germany and received the Best Paper Award at the IEEE Geoscience and Remote Sensing Symposium. He was also awarded the 2010 Distinguished Faculty Achievement Award from the University of Michigan. The IEEE Board of Directors announced him as the recipient of the 2011 IEEE Judith A. Resnik medal. In the past several years, joint papers presented by his students at a number of international symposia (IEEE APS 1995, 1997, 2000, 2001, 2003, 2005, 2006, 2007; IEEE IGARSS 1999, 2002, 2007; 2011 IEEE IMS 2001, USNC URSI 2004, 2005, 2006, 2010, 2011 AMTA 2006, URSI GA 2008) have received best paper awards.